An Improved MATLAB/Simulink Model of SiC Power MOSFETs

Gang Li
School of Electrical Engineering and Automation
Harbin Institute of Technology
Harbin, China
Email: liganghit2010@163.com

Qiang Gao
School of Electrical Engineering and Automation
Harbin Institute of Technology
Harbin, China
Email: gq651@hit.edu.cn

Miaoxin Jin
School of Electrical Engineering and Automation
Harbin Institute of Technology
Harbin, China
Email: jinmiaoxin1986@163.com

Jiabao Kou
School of Electrical Engineering and Automation
Harbin Institute of Technology
Harbin, China
Email: koujiabao_hit@163.com

Xiaolu Li
School of Electrical Engineering and Automation
Harbin Institute of Technology
Harbin, China
Email: sdlixiaolu@163.com

Diaoguo Xu
School of Electrical Engineering and Automation
Harbin Institute of Technology
Harbin, China
Email: xudiang@hit.edu.cn

***Abstract*—Simulation is always the first step in the design of power converters. To maximally make the simulation results close to the experimental results, accurate models of all passive and active elements are necessary, which are the precondition for validating the expected behavior of the complete system including its converter topology and control algorithm without any prototype. For this reason, due to the wide use of Simulink in simulation of complex systems and to avoid the physical model that is too complicated to understand for many electrical engineers, an improved model for SiC power MOSFETs based on Simulink is proposed in this paper, which is suitable for wide temperature range application from 25℃ to 200℃, even extended to lower or higher temperature easily. The static characteristics of SiC power MOSFETs are described by controllable current source whose behaviors depend on ambient temperature values. To get perfect output characteristic, a novel compensation method is presented. What's more, based on the equivalent circuit of SiC power MOSFETs, its dynamic characteristics with switching performance are analyzed in detail. The proposed model is validated with ST company's SiC power MOSFET SCT20N120 (1200V, 20A) in experimental tests.**

Keywords—SiC MOSFETs; characterization and modeling; wide temperature range; static and dynamic characteristics

I. INTRODUCTION

Almost at the same time, Si and SiC are found to be available materials in the manufacture of semiconductor devices. As for Si devices, simpler production process [1], lower cost, and meeting-demand performances make silicon devices over the past few decades has been rapid development. But with the improvement of the requirements of device performances, silicon carbide devices are becoming more and more attentive. Compared with Si devices, SiC devices have apparent advantages. Specifically, wider energy bandgap [2] makes leakage currents much lower and can operate at higher ambient temperatures. Higher critical electric field means that holding the same voltage, SiC devices can be made thinner, which results in orders-of-magnitude lower on-resistance values. SiC devices operate at higher frequencies due to higher electron saturation velocity. Higher thermal conductivity makes SiC devices can take internal thermal energy out in a timely manner to cool SiC devices themselves, so the heat sinks can be smaller or even not needed, which allows operation at higher power densities. Table 1 summarizes the key material properties of silicon and silicon carbon.

TABLE I. SUMMARY OF KEY SEMICONDUCTOR MATERIAL PROPERTIES

Parameter	*Si*	*4H-SiC*	*6H-SiC*	*3C-SiC*
Energy bandgap E_g (eV)	1.1	3.3	3	2.7
Critical electric field E_c (MV/cm)	0.3	3.5	2.5	1.5
Electron drift velocity v_{sat} (cm/s)	1E+7	2E+7	2E+7	2.5E+7
Thermal conductivity λ(W/cm-K)	1.3	3.7	3.7	3.6

Although so many significant advantages SiC devices hold, application Engineers do not understand the features of SiC

978-1-5090-1210-7/16/$31.00 ©2016 IEEE

devices clearly, especially the change of their internal parameters and external characteristics with the change of ambient temperature. Accurate SiC device model not only can greatly help the design of device driver circuit, protection circuit and EMI suppression method, but also provides guidance to series and parallel design of devices. In recent years, many scholars have proposed SiC diode models [3], SiC JFET model [4] and SiC MOSFET models [5]，[6]，[7] based on PSpice. These models are quite qualified for small circuit simulation, but can't be used for complex system simulation. Paper [8] proposes a physics-based model of a power SiC BJT, realized using MATLAB and Simulink, which has great reference significance. Paper [9] describes a SiC power MOSFET model based on MATLAB/Simulink, but the linear region error of output characteristic is difficult to accept, and the duration of miller platform is rough.

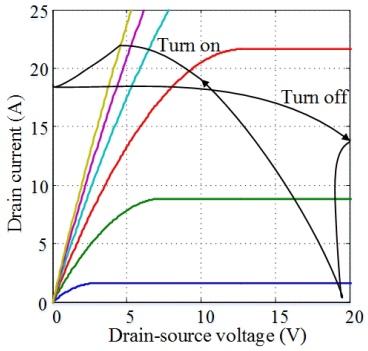

Fig. 1. Operation point trajectory in the process of switching

This paper presents an accurate SiC power MOSFET model based on MATLAB/Simulink. The static operation points of SiC MOSFET are located in cut-off region (SiC MOSFET is off) and linear region (SiC MOSFET is on). During the switching process of SiC MOSFET, the operation point goes through cut-off region, saturation region and linear region in fig.1. To ensure the accuracy of each region, a novel temperature compensation method is proposed in the static characteristics. Switching performance is analyzed in detail and an improved calculation method of miller platform duration is described in the dynamic characteristics. The results are verified by experiment measurement and test.

II. MODEL OF SiC MOSFET

Based on the widely used simulation software MATLAB/Simulink, the SiC MOSFET model can be built with the device characterization data. The important parameters about the device are obtained from simple tests and the manufacturer's datasheet [10].

A. Static characteristic

As is known, there are few study on drain current vs. drain-source voltage (I_d -V_{ds}) vertical MOSFET and also not necessary, because the research on lateral MOSFET has been so mature that we only need to do some modification for it to obtain the SiC vertical MOSFET model. The general lateral MOSFET equations [11] relating I_d-V_{ds} are explained by (1) to (3).

$$\begin{aligned} &if\ V_{gs} < V_{th} \\ &I_d = 0 \end{aligned} \tag{1}$$

$$\begin{aligned} &if\ V_{gs} > V_{th}\ \ and\ \ 0 < V_{ds} < \frac{(V_{gs} - V_{th})}{(1+a)} \\ &I_d = K \times [(V_{gs} - V_{th}) \times V_{ds} - 0.5 \times (1+a) \times V_{ds}^{\ 2}] \times (1 + \lambda \times V_{ds}) \end{aligned} \tag{2}$$

$$\begin{aligned} &if\ V_{gs} > V_{th}\ \ and\ \ V_{ds} > \frac{(V_{gs} - V_{th})}{(1+a)} \\ &I_d = \frac{K}{2 \times (1+a)} \times (V_{gs} - V_{th})^2 \times (1 + \lambda \times V_{ds}) \end{aligned} \tag{3}$$

Where $(1+\lambda \times V_{ds})$ in linear and saturation region is to consider the channel-length modulation effect. The current in the two regions is a weak function of the drain voltage. For long channel, the channel-length modulation effect is less than that of short. SiC vertical MOSFETs belong to long channel devices. Extend saturation region of I_d-V_{ds} curve in reverse to one point on the V_{ds} axis, and the negative multiplicative inverse of the point is the parameter λ. For example, in fig.2, the point on the V_{ds} axis is -20, so λ is 0.05

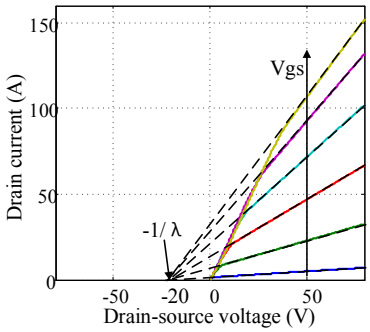

Fig. 2. Obtain parameter λ from output curves

From fig.3 and fig.4, the pinch-off voltage curves varies with the change of temperature *and* V_{gs}, and are the boundary of linear and saturation regions. The parameter a is related to the boundary. It is easy to think of calculating a with pinch-off points. The parameters a and K can be obtained by (4) to (7), where ($V_{ds\ pinch}$, $I_{d\ pinch}$) is the pinch-off point at temperature *and* V_{gs} , f_1 and f_2 is the fitting function of temperature *and* V_{gs}.

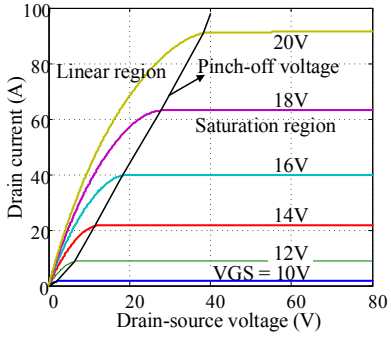

Fig. 3. Pinch-off voltage at same temperature (@25℃)

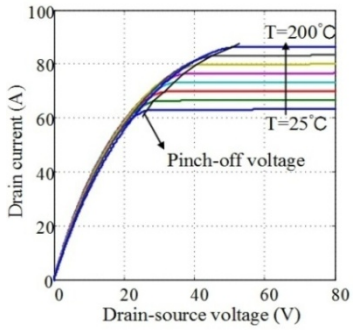

Fig. 4. Pinch-off voltage at same Vgs（18V）

$$V_{ds\_pinch} = f_1(V_{gs}, T) \tag{4}$$

$$I_{d\_pinch} = f_2(V_{gs}, T) \tag{5}$$

$$a = (V_{gs} - V_{th}) \div V_{ds\_pinch} - 1 \tag{6}$$

$$K = 2 \times I_{d\_pinch} \times (1+a) \div [(V_{gs} - V_{th})^2 \times (1 + \lambda \times V_{ds\_pinch})] \tag{7}$$

Till now, the static characteristics of a SiC MOSFET have been built, but non-ideal factors in the purity of materials and the accuracy of process. For another reason, SiC MOSFETs always operate at cut-off region and linear region. The accuracy of the model in linear region is crucial，because it has great relationship to conduction loss. To ensure accuracy, a novel compensation method is introduced. By (8) to (10), linear region at less V_{ds} is compensated. Equations (11) to (13) compensate the whole linear region slightly. The amount of compensation at the nth time is controlled by rat_n that is a function of V_{gs} and T. I_d is the basic current at V_{gs}, T and V_{ds}, and I_{compn} is current after compensation at the nth time.

$$rat_1 = f_3(V_{gs}, T) \tag{8}$$

$$k_1 = rat_1 \times (V_{ds\_pinch} - V_{ds}) \div V_{ds\_pinch} \tag{9}$$

$$I_{comp1} = I_d \times \{1 + k_1 \times [\log(1.001) - \log(V_{ds} \div V_{ds\_pinch} + 0.001)]\} \tag{10}$$

$$rat_2 = f_4(V_{gs}, T) \tag{11}$$

$$k_2 = -4 \times rat_2 \div V_{ds\_pinch}^2 \tag{12}$$

$$I_{comp2} = I_{comp1} \times [1 - k_2 \times V_{ds} \times (V_{ds} - V_{ds\_pinch})] \tag{13}$$

B. Dynamic characteristic

SiC MOSFETs with low on-resistance (R_{on}) typically operate at high frequency, thus switching loss is greater than conduction loss at a relatively high frequency. To better understand the switching process of SiC MOSFETs and contribute to the design of the drive and protection circuits of SiC MOSFETs, the research on dynamic process is very necessary.

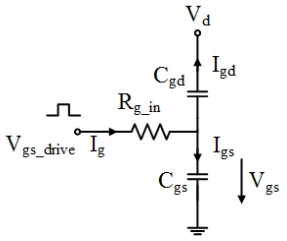

Fig. 5. An equivalent MOSFET gate circuit

To get a fundamental understanding of the switching behavior of a SiC MOSFET, a equivalent circuit of the MOSFET gate is illustrated in figure 5 after the necessary simplification, where the gate consists of an inherent resistance (R_{g_in}) and two input capacitors (C_{gd} and C_{gs}). After analysis, the output voltage response for a step gate drive voltage (V_{gs_drive}) is obtained. The output voltage response is described as (14).

$$V_{gs} = V_{gs\_drive} \times (1 - e^{-t/(C_{gs}+C_{gd}) \times R_{g\_in}}) \tag{14}$$

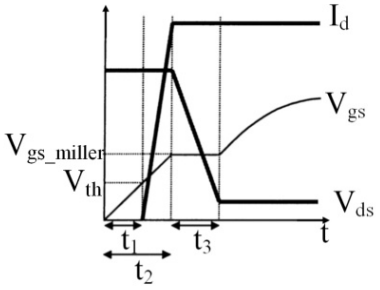

Fig. 6. Turn-on transient of MOSFETs

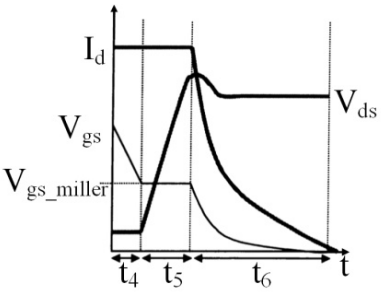

Fig. 7. Turn-off transient of MOSFETs

Both turn on and turn off processes can be divided into three stages [12], which are illustrated in figure 6 and 7. Based on above analysis, six time periods of a MOSFET about the two processes are given by (15)-(20). In order to accurately calculate t_3 and t_5, gate-drain charge is used instead of the average value of C_{gd}. Then V_{gs}, I_g, V_{ds} and I_d response for a step gate drive voltage are not difficult to calculate at every moment.

$$t_1 = (R_{g\_in} + R_{g\_out}) \times (C_{gs} + C_{gd}) \times \ln(\frac{V_{gs\_drive}}{V_{gs\_drive} - V_{th}}) \quad (15)$$

$$t_2 = (R_{g\_in} + R_{g\_out}) \times (C_{gs} + C_{gd}) \times \ln(\frac{V_{gs\_drive}}{V_{gs\_drive} - V_{gs\_miller}}) \quad (16)$$

$$t_3 = \frac{Q_{gd} \times (R_{g\_in} + R_{g\_out})}{V_{gs\_drive} - V_{gs\_miller}} \quad (17)$$

$$t_4 = (R_{g\_in} + R_{g\_out}) \times (C_{gs} + C_{gd}) \times \ln(\frac{V_{gs\_drive}}{V_{gs\_miller}}) \quad (18)$$

$$t_5 = \frac{Q_{gd} \times (R_{g\_in} + R_{g\_out})}{V_{gs\_miller}} \quad (19)$$

$$t_6 = (R_{g\_in} + R_{g\_out}) \times (C_{gs} + C_{gd}) \times \ln(\frac{V_{gs\_miller}}{V_{th}}) \quad (20)$$

III. SIMULATION AND EXPERIMENTAL RESULTS

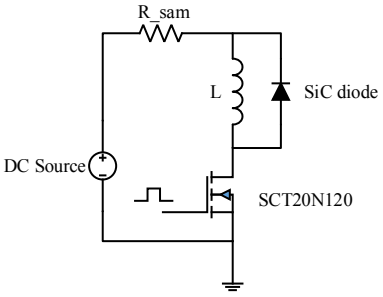

Fig. 8. Test circuit with inductive load

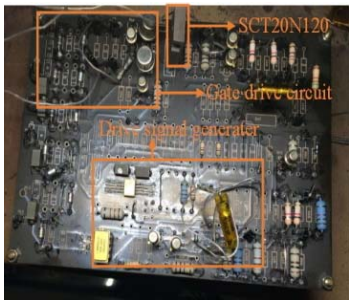

Fig. 9. Testing platform

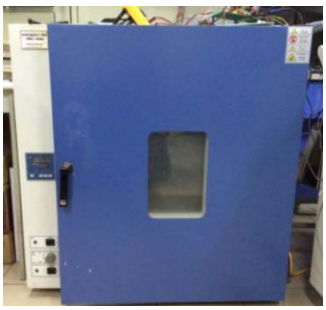

Fig. 10. Temperature programmable experiment box

Before To evaluate the proposed model, a test circuit is employed that is illustrated in figure 8, where the sampling resistor is 1.3Ω. Figure 9 and 10 show the test platform and figure 11 presents the block of proposed model. The results of simulation are compared with that of experiment. In figure 12, the transfer characteristic curves evaluated for T=25℃, T=100℃, T=150℃ and T=200℃.

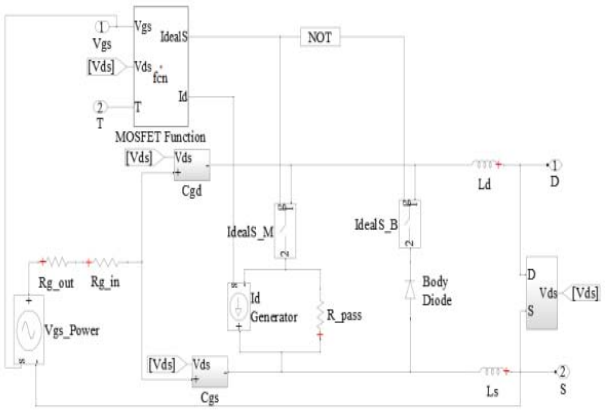

Fig. 11. The block of proposed model

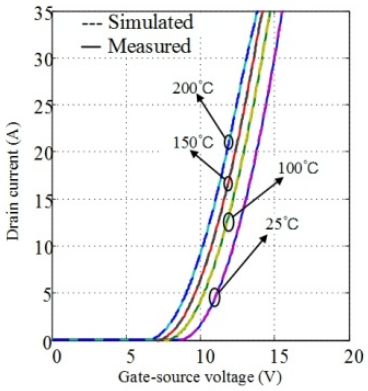

Fig. 12. Transfer curves

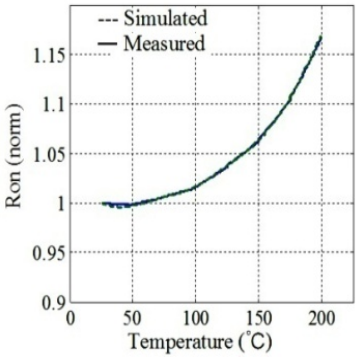

Fig. 13. Normalized on-resistance

From figure 13, on-resistance is a weak function of temperature which makes SiC MOSFETs excellent high temperature properties. The output characteristic curves are

parameterized for applied gate voltage V_{gs}=10V-20V and temperature at 25℃，100℃ and 200℃ in figures 14-16.

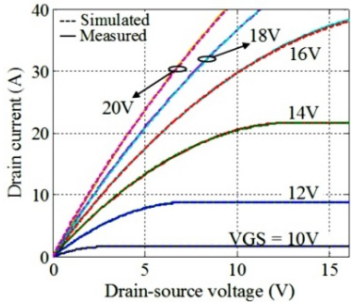

Fig. 14. I_d-V_{ds} curves at 25℃

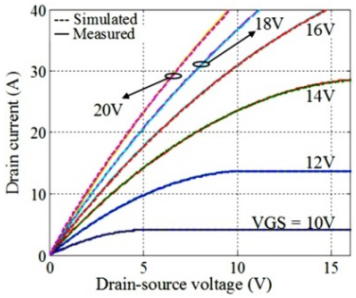

Fig. 15. I_d-V_{ds} curves at 100℃

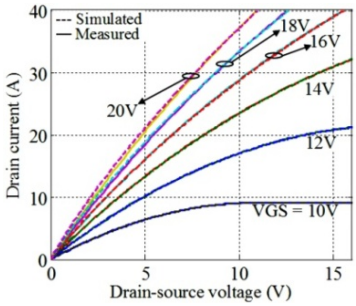

Fig. 16. I_d-V_{ds} curves at 200℃

The switching characteristics of the SiC MOSFET were also measured under room temperature. The drive voltage applied was 0-14.5V. Figure17 shows the typical turn-on and turn-off transients of the gate voltage V_{gs} and gate current I_g, the drain-source voltage V_{ds}, as well as the drain current I_d. The simulation results in figure 18 are compared with experiments'.

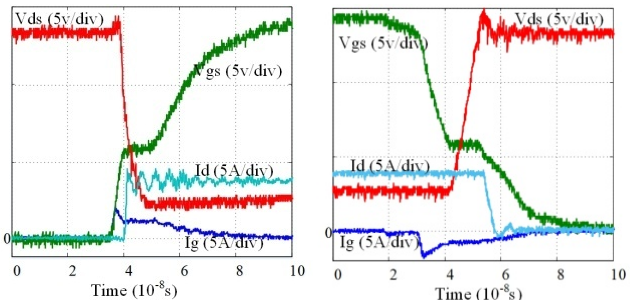

Fig. 17. Switching performance from experiment

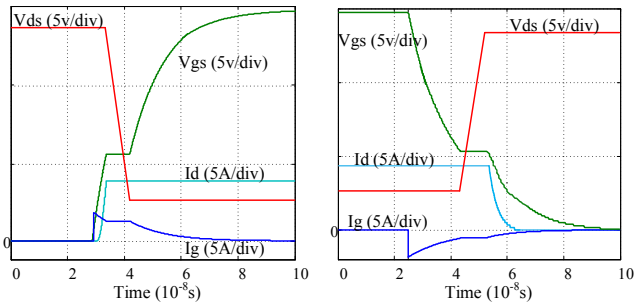

Fig. 18. Switching performance from simulation

IV. CONCLUSION

The key characteristics of a vertical SiC MOSFET have been intensively investigated. After reasonable modifications of the conventional Si power MOSFETs' behaviors, a simple but accurate Matlab/Simulink model for a vertical SiC MOSFET is proposed to predict the actual application behaviors. The static characteristics show that SiC MOSFETs always keep a lower on-resistance in blocking high voltage and R_{on} increases more slowly with ambient temperature climbing than Si MOSFETs. Taking into account some discrepancies those are inevitable in experiment, the proposed model successfully simulated the device's switching performance, which can be used to estimate switching losses. The discussions presented in this paper are very helpful for the design of gate drive circuit and protection circuit, and contribute to develop and build future models for SiC power devices.

REFERENCES

[1] Burk, A.A.; O'Loughlin, M.J.; Garrett, L.S., "Silicon carbide materials for advanced power electronic devices," in Semiconductor Device Research Symposium, 2009. ISDRS '09. International , vol., no., pp.1-2, 9-11 Dec. 2009

[2] Stevanovic, L.D.; Matocha, K.S.; Losee, P.A.; Glaser, J.S.; Nasadoski, J.J.; Arthur, S.D., "Recent advances in silicon carbide MOSFET power devices," in Applied Power Electronics Conference and Exposition (APEC), 2010 Twenty-Fifth Annual IEEE , pp.401-407, 21-25 Feb. 2010

[3] Ruiyun Fu; Grekov, A.E.; Kang Peng; Santi, E., "Parameter Extraction Procedure for a Physics-Based Power SiC Schottky Diode Model," in Industry Applications, IEEE Transactions on , vol.50, no.5, pp.3558-3568, Sept.-Oct. 2014

[4] Funaki, T.; Kashyap, A.S.; Mantooth, H.A.; Balda, J.C.; Barlow, F.D.; Kimoto, T.; Hikihara, T., "Characterization of SiC JFET for Temperature Dependent Device Modeling," in Power Electronics Specialists Conference, 2006. PESC '06. 37th IEEE , pp.1-6, 18-22 June 2006

[5] Jun Wang; Tiefu Zhao; Jun Li; Huang, A.Q.; Callanan, R.; Husna, F.; Agarwal, A., "Characterization, Modeling, and Application of 10-kV SiC MOSFET," in Electron Devices, IEEE Transactions on , vol.55, no.8, pp.1798-1806, Aug. 2008

[6] Kai Sun; Hongfei Wu; Juejing Lu; Yan Xing; Lipei Huang, "Improved Modeling of Medium Voltage SiC MOSFET Within Wide Temperature Range," in Power Electronics, IEEE Transactions on , vol.29, no.5, pp.2229-2237, May 2014

[7] Mudholkar, M.; Ahmed, S.; Ericson, M.N.; Frank, S.S.; Britton, C.L.; Mantooth, H.A., "Datasheet Driven Silicon Carbide Power MOSFET Model," in Power Electronics, IEEE Transactions on , vol.29, no.5, pp.2220-2228, May 2014

[8] Gachovska, T.; Hudgins, J.L.; Bryant, A.; Santi, E.; Mantooth, H.A.; Agarwal, A.K., "Modeling, Simulation, and Validation of a Power SiC BJT," in Power Electronics, IEEE Transactions on , vol.27, no.10, pp.4338-4346, Oct. 2012

[9] Paolo Giammatteo; Concettina Buccella; Carlo Cecati, "Matlab/Simulink Modeling of SiC Power MOSFETs," in International Review of Electrical Engineering, vol.9, no.4, pp.671-680, July 2014.

[10] 1200V-20A SiC Power MOSFET SCT20N120 Datasheet, http://www.st.com/web/cn/home/catalog/sense_power/FM100/CL2062/SC1704/PF260608.

[11] Pratap, R.; Singh, R.K.; Agarwal, V., "SPICE model development for SiC power MOSFET," in Power Electronics, Drives and Energy Systems (PEDES), 2012 IEEE International Conference on, pp.1-5, 16-19 Dec. 2012.

[12] Brown, J., "Modeling the switching performance of a MOSFET in the high side of a non-isolated buck converter," in Power Electronics, IEEE Transactions on , vol.21, no.1, pp.3-10, Jan. 2006 doi: 10.1109/TPEL.2005.861110